Journal of Sound and Vibration 333 (2014) 2073–2086

Contents lists available at ScienceDirect

Journal of Sound and Vibration

journal homepage: www.elsevier.com/locate/jsvi

Introducing a Green–Volterra series formalism to solve weakly nonlinear boundary problems: Application to Kirchhoff's string

David Roze [a,b,*], Thomas Hélie [a,b]

[a] CNRS, UMR 9912, IRCAM, 1 place Igor Stravinsky, F-75004, Paris, France
[b] Sorbonne Universités, UPMC Univ Paris 06, UMR 9912, IRCAM, F-75004, Paris, France

ARTICLE INFO

Article history:
Received 3 May 2012
Received in revised form
4 November 2013
Accepted 12 November 2013
Handling Editor: L.N. Virgin
Available online 22 December 2013

ABSTRACT

This paper introduces a formalism which extends that of "Green's function" and that of "the Volterra series". These formalisms are typically used to solve, respectively, linear inhomogeneous space–time differential equations in physics and weakly nonlinear time-differential input-to-output systems in automatic control. While Green's function is a space–time integral kernel which fully characterizes a linear problem, the Volterra series expansions involve a sequence of multi-variate time integral kernels (of convolution type for time-invariant systems). The extension proposed here consists in combining the two approaches, by introducing a series expansion based on multi-variate space–time integral kernels. This series allows the representation of the space–time solution of weakly nonlinear boundary problems excited by an "input" which depends on space and time.

This formalism is introduced on and applied to a nonlinear model of a damped string that is excited by a transverse mass force $f(x,t)$. The Green–Volterra kernels that solve the transverse displacement dynamics are computed. The first-order kernel exactly corresponds to Green's function of the linearized problem. The higher order kernels satisfy a sequence of linear boundary problems that lead to (both) analytic closed-form solutions and modal decompositions. These results lead to an efficient simulation structure, which proves to be as simple as the one based on the Volterra series, that has been obtained in a previous work for excitation forces with separated variables $f(x,t)=\phi(x)f_{\mathrm{tot}}(t)$. Numerical results are presented.

1. Introduction

Sound synthesis based on physical models makes use of dynamical models of resonators that must be accurate enough to be realistic. Many models are available for strings, plates, pipes (see e.g. [1–10]). In addition to basic (conservative) wave propagation, these models include some relevant second-order phenomena such as nonlinearities that are responsible for the timbre variation with respect to the nuance (from pp to ff) and damping.

In this context, simulation methods are also an important issue. The Volterra series formalism [11] provides a convolution-type solution for "weakly nonlinear systems", from which simple simulation structures can be derived and are available for bounded input signals. More precisely, it extends linear filtering (impulse response and transfer

* Corresponding author.
E-mail addresses: david.roze@ircam.fr (D. Roze), thomas.helie@ircam.fr (T. Hélie).

0022-460X/$ - see front matter © 2013 Elsevier Ltd. All rights reserved.
http://dx.doi.org/10.1016/j.jsv.2013.11.024

function) to the case of systems with distortions, the dynamics of which can be represented by a sum of multiple convolutions (multi-variate kernels and transfer kernels). For this reason, this tool has been widely used in e.g. signal processing, automatic control, electronics, mechanics (see e.g. [12–20]).

In a previous work [21], a nonlinear equation of a damped string has been solved using the Volterra series in the case where the string is excited by a force $f_{\text{tot}}(t)$ which is spatially distributed by a time-invariant function $\phi(x)$. Thus, a time-domain simulation of the transverse displacement $u(x,t)$ has been derived from the truncated series, which provides accurate results for all signal input $f_{\text{tot}}(t)$ with sufficiently small amplitudes. In practice, for sound synthesis issues (bowed string, pinched string, etc), the main limitation of this solution is due to the time-invariance of the spatial distribution ϕ. In the linear case, for a general space–time transverse mass force $f(x,t)$, this problem is solved by using Green's function which fully characterizes the considered system.

In this paper, we introduce a "Green–Volterra" formalism which extends both that of "Green's function" and that of "the Volterra series". Applying this formalism to the string allows one to compute its dynamics whatever the excitation force $f(x,t)$ may be. The solution is given by a series expansion composed of space–time integrals involving the (computable) "Green–Volterra" kernels. The first term of the series expansion exactly corresponds to Green's function solution. Higher order terms introduce nonlinear dynamics contributions.

The paper is organized as follows. Section 2 introduces the nonlinear string model. It recalls results based on Green's function for the linearized problem (Section 2.2) and based on the Volterra series for a particular class of excitations (Section 2.3). Section 3 introduces the formalism of Green–Volterra series. Then, this formalism is used to solve the original problem in Section 4. A simulation is deduced in Section 5. Finally, Section 6 develops conclusions and perspectives.

2. Problem statement

2.1. Model under consideration

Consider the dimensionless nonlinear Kirchhoff model of the transverse vibrations of a damped string [2] excited by a force f distributed on $\Omega=]0,1[$ given by, for all $(x,t)\in\Omega\times\mathbb{R}_+$,

$$\partial_t^2 u(x,t)+2\alpha\partial_t u(x,t)-\left(1+\varepsilon\left[\int_\Omega(\partial_x u(x,t))^2\,\mathrm{d}x\right]\right)\partial_x^2 u(x,t)=f(x,t), \tag{1}$$

with Dirichlet boundary conditions and zero initial conditions

$$\forall t>0,\quad u(x=0,t)=0\quad\text{and}\quad u(x=1,t)=0, \tag{2}$$

$$\forall x\in\Omega,\quad u(x,t=0)=0\quad\text{and}\quad \partial_t u(x,t=0)=0. \tag{3}$$

Coefficients ε and α are positive. They quantify the effects of the nonlinearity (due to the variation of tension) and of the fluid damping (due to viscosity, see e.g. [22, p. 194]).

2.2. Linearized problem: Green's function solution

The linearized version of (1)–(3) is obtained for $\varepsilon=0$. It has the form

$$L_{x,t}[u]=f, \tag{4}$$

where $L_{x,t}$ is the linear differential operator $\partial_t^2+2\alpha\partial_t-\partial_x^2$ over the domain $(x,t)\in\Omega\times\mathbb{R}_+$ associated with Dirichlet boundary conditions and zero initial conditions. This standard well-posed problem has been extensively studied.

In general, boundary linear problems governed by Eq. (4) can be solved using Green's function formalism [23,24] (see also e.g. [22,25] for applications in musical acoustics): the solution is the superposition of all local contributions of f, given by the integral

$$u(x,t)=\int_{\Omega\times\mathbb{R}_+} g(x,t;\xi,\tau)f(\xi,\tau)\,\mathrm{d}\xi\,\mathrm{d}\tau, \tag{5}$$

where Green's kernel g denotes the solution of Eq. (4) excited by the Dirac pulse centered at (ξ,τ), that is,

$$f(x,t)=[\delta_\xi\otimes\delta_\tau](x,t)=\delta(x-\xi)\delta(t-\tau), \tag{6}$$

where $\otimes$ denotes the tensor product of two distributions [26, Chapter 3.1].

Note that this problem is time invariant but not space invariant so that $g(x,t;\xi,\tau)=g(x,0;\xi,\tau-t)$. Indeed, denote by $T_{(\tau,\xi)}$ the translation operator of duration τ and length ξ. If (f,u) is a solution, it appears that $(T_{(\tau,0)}f,T_{(\tau,0)}u)$ is also a solution (time-invariance), because $T_{(\tau,0)}$ commutes with all the operators of the partial differential equation, whereas $(T_{(0,\xi)}f,T_{(0,\xi)}u)$ is not. Hence, Eq. (5) becomes a convolution w.r.t. time, that is,

$$u(x,t)=\int_{\Omega\times\mathbb{R}_+}\underline{g}(x;\xi,\tau)f(\xi,t-\tau)\,\mathrm{d}\xi\,\mathrm{d}\tau\quad\text{where }\underline{g}(x;\xi,\tau)=g(x,0;\xi,-\tau).$$

denotes the convolution-type Green's kernel.

In the Laplace domain, the linear boundary problem (1)–(3) can be written as, for all $s \in \mathbb{C}_0^+ = \{s \in \mathbb{C} | \mathrm{Re}(s) > 0\}$,

$$\Gamma^2 U - \partial_x^2 U = F \quad \text{on the string } (x \in \Omega), \tag{7}$$

and

$$U = 0 \quad \text{at boundaries } (x \in \{0, 1\}), \tag{8}$$

where $F(x,s)$ and $U(x,s)$ denote the Laplace transforms (with respect to variable t) of f and u, respectively, and

$$\text{for all } s \in \mathbb{C}_0^+, \quad \Gamma(s) = \sqrt{s^2 + 2\alpha s}, \tag{9}$$

where $z \mapsto \sqrt{z}$ is the principal value of the square root (that is, the analytic continuation over $\mathbb{C}\backslash\mathbb{R}_-$ of the positive square root on $\mathbb{R}_+$.

It solves into, for all $(x,s) \in \Omega \times \mathbb{C}_0^+$ and $\xi \in \Omega$,

$$U(x,s) = \int_\Omega G(x;\xi,s) F(\xi,s)\, \mathrm{d}\xi, \tag{10}$$

$$G(x;\xi,s) = \frac{\cosh((1+x+\xi)\Gamma(s)) - \cosh((1-|x-\xi|)\Gamma(s))}{2\Gamma(s)\sinh(\Gamma(s))}, \tag{11}$$

where G corresponds to the Laplace transform of $\underline{g}$ w.r.t. t. For $(x,\xi) \in \Omega^2$, function $s \mapsto G(x;\xi,s)$ is analytic on $\mathbb{C}_0^+$. It corresponds to the transfer function of a causal strictly stable input-to-output system.

This solution can also be decomposed into the eigenfunctions $\{e_k\}_{k \in \mathbb{N}^*}$ where $e_k(x) = \sqrt{2}\sin(k\pi x)$, which define an orthonormal basis of $L^2(\Omega)$. Thus, introducing

$$U(x,s) \underset{L^2(\Omega)}{=} \sum_{k \in \mathbb{N}^*} U_k(s) e_k(x) \quad \text{where } U_k(s) = \langle U(\cdot,s), e_k(\cdot)\rangle_{L^2(\Omega)}, \tag{12}$$

and using similar definitions for F, Eqs. (7) and (8) are solved if $[\Gamma(s)^2 + (k\pi)^2]U_k(s) = F_k(s)$, that is,[1]

$$U_k(s) = G^{[k]}(s) F_k(s) \quad \text{where } G^{[k]}(s) = \frac{1}{s^2 + 2\alpha s + k^2\pi^2}. \tag{13}$$

If $\alpha < \pi$, then the characteristic equation of the k-th mode ($\Gamma(s)^2 + k^2\pi^2 = 0$) admits a pair of complex conjugate roots $(\lambda_k, \overline{\lambda_k})$ with $\lambda_k = -\alpha + \mathrm{i}\sqrt{\omega_k}$ and $\omega_k = \sqrt{k^2\pi^2 - \alpha^2} > 0$. The modal decomposition yields, in the time domain,

$$u(x,t) = \sum_{k=1}^{+\infty} \left[\underline{g}^{[k]} \star f_k\right](t) e_k(x) \quad \text{with } \underline{g}^{[k]}(t) = \frac{\sin(\omega_k t)}{\omega_k} \mathrm{e}^{-\alpha t} Y(t), \tag{14}$$

where $\star$ is the standard convolution operator and Y denotes the Heaviside step function.

For sound synthesis purposes, real-time simulations are often based on a truncated version of this modal decomposition [27]. The block-diagram corresponding to Eqs. (12)–(14) truncated at order K is displayed in Fig. 1. For simulations, digital versions of filters with transfer function $G^{[k]}(s)$ are implemented, based on second-order auto-regressive digital filters.

2.3. Simulation of a nonlinear problem with Volterra series

The nonlinear problem (1)–(3) has been solved in [21] in the case where

$$f(x,t) = [\phi \otimes f_{\mathrm{tot}}](x,t) = \phi(x) f_{\mathrm{tot}}(t), \tag{15}$$

using the Volterra series expansion: the solution is decomposed into homogeneous nonlinear contributions as

$$u(x,t) = \sum_{n=1}^{+\infty} \int_{\mathbb{R}^n} h_n^{(x)}(\tau_1, \ldots, \tau_n) f_{\mathrm{tot}}(t-\tau_1) \ldots f_{\mathrm{tot}}(t-\tau_n)\, \mathrm{d}\tau_1 \ldots \mathrm{d}\tau_n. \tag{16}$$

Each term of the series corresponds to a multiple time-convolution of repeated versions of f_{tot} with kernels $h_n^{(x)}$: $n=1$ isolates the linear contribution on the dynamics due to f_{tot} (with its memory effect), $n=2$ isolates the quadratic one, etc. The Volterra kernels are parameterized by the space variable x. They can be given by the modal decomposition

$$h_n^{(x)}(\tau_1, \ldots, \tau_n) = \sum_{k=1}^{+\infty} h_n^{[k]}(\tau_1, \ldots, \tau_n) e_k(x) \quad \text{with } h_1^{[k]} = \phi_k \underline{g}^{[k]} \quad \text{and, for } n \geq 2,\ h_n^{[k]} = \underline{g}^{[k]} \star^n r_n^{[k]}.$$

In this equation, function $\underline{g}^{[k]}$ is defined in Eq. (14). Constant ϕ_k is the projection of ϕ on e_k, that is, $\phi_k = \langle \phi, e_k \rangle_{L^2(\Omega)}$. Function r_n is a combination[2] of kernels $h_j^{[k]}$ with $j < n$. Moreover, symbol $\star^n$ denotes the convolution-type operator $[a \star^n b_n](\tau_1, \ldots, \tau_n) = \int_{\mathbb{R}} a(\theta) b_n(\tau_1 - \theta, \ldots, \tau_n - \theta)\, \mathrm{d}\theta$.

[1] The square brackets in $G^{[k]}$ and used further in the paper are introduced to avoid confusion between superscripting and raising into power.

[2] The exact equation is given by $r_n^{[k]}(\tau_1, \ldots, \tau_n) = -\varepsilon k^2 \pi^4 \sum_{m_1 + m_2 + m_3 = n} \left[\sum_{\ell \in \mathbb{N}^*} \ell^2 h_{m_1}^{[\ell]}(\tau_1, \ldots, \tau_{m_1}) h_{m_2}^{[\ell]}(\tau_{m_1+1}, \ldots, \tau_{m_1+m_2})\right] \times h_{m_3}^{[k]}(\tau_{m_1+m_2+1}, \ldots, \tau_n)$.

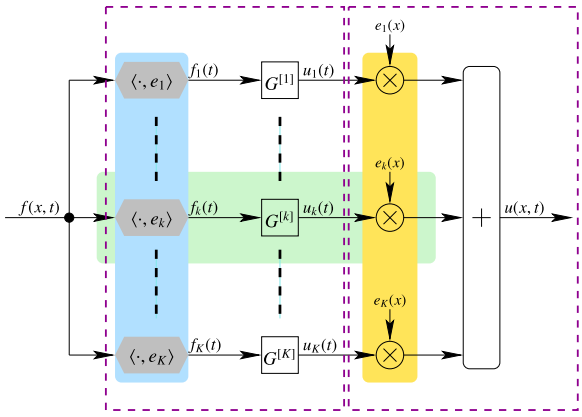

Fig. 1. Block-diagram of the simulation of the linearized version of (1)–(3) with K modes. Symbol $\otimes$ is a standard multiplication. More precisely, for functions with separated variables ($x\mapsto e_k(x)$ and $t\mapsto u_k(t)$), it corresponds to the tensor product $[e_k\otimes u_k](x,t)=e_k(x)u_k(t)$ as in Eq. (6).

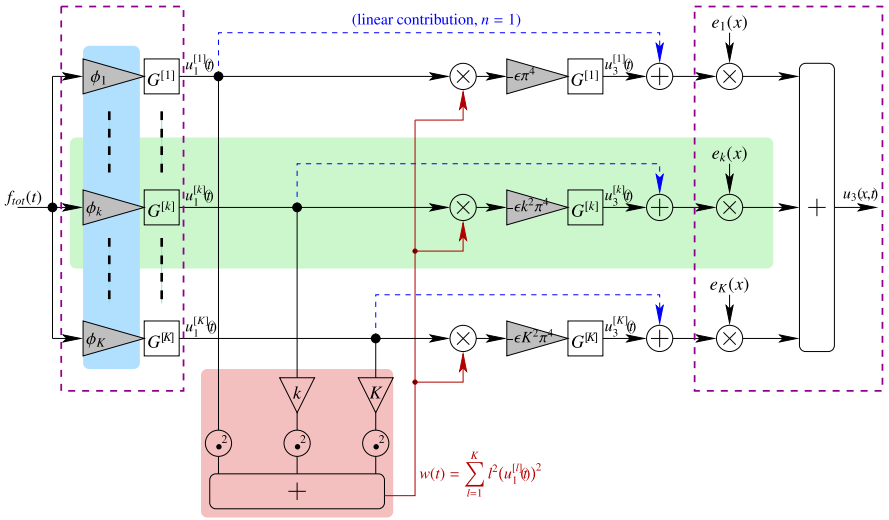

Fig. 2. Block-diagram of an $o(\varepsilon)$−simulation of Eq. (1) with K modes: the dashed arrows isolate the linear dynamics ($n=1$) of each mode; the shaded central part isolates the $o(\varepsilon)$−dynamics of a mode k; the shaded bottom part isolates the dynamics of the integral term in Eq. (1); the shaded left part corresponds to simple gains, controlled by the spatial distribution of the excitation force. Note that the two dotted boxes correspond to those in Fig. 1 since $\phi_k=\langle\phi,e_k\rangle_{L^2(\Omega)}$.

If excitations only involve the K first modes ($\phi_k=0$ if $k\geq K+1$), this expansion truncated at order 3 corresponds to the block-diagram displayed in Fig. 2 (see [21, Section 4] for the detailed computation of kernels and the equivalent realization into block-diagrams).

The question addressed below is

> *"How to solve the nonlinear problem Eqs. (1)–(3) for a general excitation $f(x,t)$, that is, when f is not limited to the case $f(x,t)=\phi(x)f_{\rm tot}(t)$?"*

An intuitive solution would consist in replacing $f_{\rm tot}$ and ϕ_k in Fig. 2 by f and $\langle\cdot,e_k\rangle$, respectively, as in Fig. 1. This result is actually the one which is obtained thanks to the formalism proposed below. This formalism combines that of Green's functions (as for Fig. 1) and that of the Volterra series (as for Fig. 2).

3. Introduction to the Green–Volterra series

3.1. Preamble: regular perturbation theory and formal series expansion

Consider an inhomogeneous differential equation defined on a domain $(x,t)\in\Omega\times\mathbb{T}$ (with $\mathbb{T}=\mathbb{R}$ or with $\mathbb{T}=\mathbb{R}_+$ and zero initial conditions), which is excited by f and governed by

$$L_{x,t}[u]=f+K_{x,t}[u,f]. \tag{17}$$

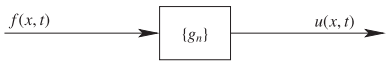

Fig. 3. System represented by its Green–Volterra kernels.

In Eq. (17), $L_{x,t}$ is a linear operator w.r.t. space x and time t and $K_{x,t}$ is a sum of multilinear operators $K_{x,t}^{p,q}$, that is,

$$K_{x,t}[u,f] = \sum_{\substack{p,q \geq 0 \\ p+q \geq 2}} K_{x,t}^{p,q}\left[\underbrace{u,\dots,u}_{p},\underbrace{f,\dots,f}_{q}\right]. \tag{18}$$

Consider f as a perturbation and mark it by $\eta > 0$ through the change of variable $f = \eta\tilde{f}$. Following the regular perturbation method (see e.g. [28, Chapter 5]), write the solution as a power series w.r.t. η and substitute u and f into Eqs. (17) and (18) by this series $\sum_{n\in\mathbb{N}}\eta^n\tilde{u}_n$ and $\eta\tilde{f}$, respectively. Then, exploiting the multilinearity of $K_{x,t}^{p,q}$ to sort the contributions w.r.t. η^n, we formally obtain a sequence of linear problems. Choosing $\eta = 1$ to remove the tilde symbols, this yields $u_0 = 0$ and for $n \geq 1$,

$$L_{x,t}[u_n] = \kappa_n \quad \text{with } \kappa_1 = f \tag{19}$$

and

$$\kappa_n = \sum_{\substack{(p,q)\in[0,n]^2_{\mathbb{N}} \\ 2\leq p+q\leq n}} \sum_{\substack{m\in(\mathbb{N}^*)^p \\ m_1+\cdots+m_p=n-q}} K_{x,t}^{p,q}\left[\underbrace{u_{m_1},\dots,u_{m_p}}_{p},\underbrace{f,\dots,f}_{q}\right] \quad \text{if } n \geq 2. \tag{20}$$

If g is Green's function of Eq. (19) in the space–time domain, it comes that

$$u_n(x,t) = \int_{\Omega\times\mathbb{T}} g(x,t;\xi,\tau)\kappa_n(\xi,\tau)\,\mathrm{d}\xi\,\mathrm{d}\tau. \tag{21}$$

Deriving the series $u = \sum_{n\in\mathbb{N}}u_n$, we finally find that u can formally be expressed as a sum over $n \in \mathbb{N}^*$ of multiple integrals on n repeated versions of f combined with multi-variate kernels. In the present case, these kernels define the *Green–Volterra* kernels introduced below. Such kernels can be found in e.g. [29].

Remark 1 (*Volterra series*). For a finite-dimensional time-differential system, these kernels only depend on time variables t and τ. They define a so-called Volterra series (see e.g. [11,14]). Moreover, if the system is time-invariant, they are of convolution type.

Remark 2 (*About Green's principle*). As mentioned in Section 2.2 for linear problems (see Eq. (5)), Green's principle relies on the superposition principle: the solution of a sum of elementary excitations is the sum of the solutions of each excitation, considered separately. Note that the perturbation method does not preserve this principle, which is obviously void for nonlinear problems. Indeed, Eq. (20) begets a coupling of each elementary excitation through multilinear operators $K_{x,t}^{p,q}$.

3.2. Definition of Green–Volterra series and basic properties

Definition 1 (*Green–Volterra series*). A system with input $f(x,t)$ and output $u(x,t)$, defined on domain $\Omega\times\mathbb{T}$, is described by a Green–Volterra series of kernels $\{g_n\}_{n\in\mathbb{N}^*}$ (see Fig. 3), if

$$u(x,t) = \sum_{n=1}^{+\infty}\int_{\Omega^n\times\mathbb{T}^n} g_n(x,t;\boldsymbol{\xi},\boldsymbol{\tau})f(\xi_1,\tau_1)\dots f(\xi_n,\tau_n)\,\mathrm{d}\boldsymbol{\xi}\,\mathrm{d}\boldsymbol{\tau}, \tag{22}$$

where, for each $n \in \mathbb{N}^*$, bold symbols $\boldsymbol{\xi}$ and $\boldsymbol{\tau}$ denote (in each kernel g_n, without ambiguity) the two n-tuples $\boldsymbol{\xi} = (\xi_1,\dots,\xi_n)$ and $\boldsymbol{\tau} = (\tau_1,\dots,\tau_n)$, and where $\mathrm{d}\boldsymbol{\xi}$ and $\mathrm{d}\boldsymbol{\tau}$ are the corresponding Lebesgue measures.

Remark 3 (*Examples*). Green–Volterra series embed systems described by

(a) linear problems: kernel g_1 is Green's function and, for $n \geq 2$, kernels g_n are zero;
(b) power series functions $u = g(f) = \sum_{n=1}^{+\infty}\gamma_n f^n$ such that $g(0) = 0$: kernels are the multi-variate Dirac distributions $g_n(x,t;\boldsymbol{\xi},\boldsymbol{\tau}) = \gamma_n\delta_{x,t}^n(\boldsymbol{\xi},\boldsymbol{\tau})$, weighted by γ_n, centered at x for variables of ξ, and at t for variables of τ, that is,[3]

$$\delta_{x,t}^n(\boldsymbol{\xi},\boldsymbol{\tau}) = \left[\underbrace{\delta_x\otimes\cdots\otimes\delta_x}_{n}\otimes\underbrace{\delta_t\otimes\cdots\otimes\delta_t}_{n}\right](\xi_1,\dots,\xi_n,\tau_1,\dots,\tau_n)$$

[3] More rigorously, $g_n(x,t;\boldsymbol{\xi},\boldsymbol{\tau})\,\mathrm{d}\boldsymbol{\xi}\,\mathrm{d}\boldsymbol{\tau}$ should be written as $\gamma_n M_{x,t}(\mathrm{d}\boldsymbol{\xi},\mathrm{d}\boldsymbol{\tau})$ where $M_{x,t}$ is the multi-variate Dirac distribution (still centered at x,t).

$$= \delta(\xi_1 - x)\ldots\delta(\xi_n - x)\delta(\tau_1 - t)\ldots\delta(\tau_n - t); \tag{23}$$

(c) their various combinations (sum, product, multilinear maps, cascade) detailed in Section 3.3.

A well-posed condition for the convergence (similar to [30, Section 2.2] for the Volterra series) is given for kernels such that $(x,t) \in \Omega \times \mathbb{T} \mapsto ((\boldsymbol{\xi},\boldsymbol{\tau}) \in \Omega^n \times \mathbb{T}^n \mapsto g_n(x,t;\boldsymbol{\xi},\boldsymbol{\tau})) \in \mathcal{G}_n = L^\infty(\Omega \times \mathbb{T}, L^1(\Omega^n \times \mathbb{T}^n, \mathbb{R}))$, as follows.

Property 1 (*Gain bound function φ_g and convergence*). *If the convergence radius ρ_g of*

$$\varphi_g(z) = \sum_{n=1}^{+\infty} \|g_n\|_{\mathcal{G}_n} z^n$$

is positive, then for all bounded excitation f such that $\|f\|_\infty < \rho_g$, the Green–Volterra series (22) converges in norm in $L^\infty(\Omega \times \mathbb{T}, \mathbb{R})$. Moreover, in this case, u is also bounded and

$$\|u\|_\infty \le \varphi_g(\|f\|_\infty).$$

The proof is straightforward, remarking that each term u_n of the series expansion (22) is such that $\|u_n\|_\infty \le \|g_n\|_{\mathcal{G}_n}(\|f\|_\infty)^n$.

Remark 4 (*Convergence and truncation order for applications*). This result is limited in practice. First, spaces $\mathcal{G}_n$ include neither finite-energy spaces (or their Sobolev versions, adapted to many physical problems) nor distributions as in Example 3(b). However, some existence and uniqueness conditions of problems (17) and (18) can be found in [31], which are not limited to L^∞ spaces. Second, even if $g_n \in \mathcal{G}_n$, estimating $\|g_n\|_{\mathcal{G}_n}$ and ρ_g is usually not straightforward.

Because of these technical difficulties, convergence is not examined below. For the computation of convergence bounds, we refer to [32–33]: these works detail results for trajectories belonging to some Banach spaces and include truncation error bounds. Here, the truncation order is chosen to be low ($N=5$ in Section 4) and, in practice, we consider inputs such that the magnitude of u_n decreases with n till N.

Property 2 (*Translational symmetries, causality and transfer kernels*).

(i) *If a problem is invariant under space translations, then $g_n(x,t;\boldsymbol{\xi},\boldsymbol{\tau}) = g_n(0,t;\boldsymbol{\xi}-x,\boldsymbol{\tau})$ where $\boldsymbol{\xi}-x = (\xi_1-x,\ldots,\xi_n-x)$.*
(ii) *If a problem is time-invariant, then $g_n(x,t;\boldsymbol{\xi},\boldsymbol{\tau}) = g_n(x,0;\boldsymbol{\xi},\boldsymbol{\tau}-t)$ and we introduce the convolution-type kernel*

$$\underline{g}_n(x;\boldsymbol{\xi},\boldsymbol{\theta}) = g_n(x,0;\boldsymbol{\xi},-\boldsymbol{\theta}),$$

so that Eq. (22) becomes $u(t) = \sum_{n=1}^{+\infty} \int_{\Omega^n \times \mathbb{T}^n} \underline{g}_n(x;\boldsymbol{\xi},\boldsymbol{\theta}) f(\xi_1, t-\theta_1)\ldots f(\xi_n, t-\theta_n)\, \mathrm{d}\boldsymbol{\xi}\, \mathrm{d}\boldsymbol{\theta}$.
(iii) *If a problem is causal, then g_n is zero as soon as $\max(\boldsymbol{\tau}) > t$ (or, $\min \boldsymbol{\theta} < 0$).*

Moreover, for causal time-invariant systems (ii) and (iii), we introduce the Green–Volterra transfer kernel G_n defined by the multivariate mono-lateral Laplace transform

$$G_n(x;\boldsymbol{\xi},\boldsymbol{s}) = \int_{\mathbb{R}_+^n} \underline{g}_n(x;\boldsymbol{\xi},\boldsymbol{\tau}) \mathrm{e}^{-(s_1\tau_1 + \cdots + s_n\tau_n)}\, \mathrm{d}\boldsymbol{\tau}, \tag{24}$$

for all complex multiple variables $\boldsymbol{s} = (s_1,\ldots,s_n)$ such that the integral is absolutely convergent. For stable systems, this domain includes $(\mathbb{C}_0^+)^n$ where $\mathbb{C}_0^+ = \{s \in \mathbb{C} | \mathrm{Re}(s) > 0\}$.

Eq. (24) gives a generalization of function $G(=G_1)$ defined in Section 2.2 (see also Example 3(a)). Other properties, introduced below, deal with combinations of Green–Volterra series (we refer to e.g. [14,30,35] for corresponding results about the Volterra series). They are used to compute the Green–Volterra kernels of the string in Section 4.

3.3. Interconnection laws

Consider several systems defined by the Green–Volterra series $\{a_n\}_{n\in\mathbb{N}^*}$, $\{b_n\}_{n\in\mathbb{N}^*}$ and $\{a_n^{[\ell]}\}_{n\in\mathbb{N}^*}$ for $1 \le \ell \le j$. Then, the Green–Volterra series $\{g_n\}_{n\in\mathbb{N}^*}$ of the systems described in Fig. 4(a–c) can be derived: kernels g_n and the corresponding transfer kernels G_n for time-invariant causal systems are given.

Case (a): sum (the radius of convergence ρ_g is such that $\rho_g \ge \min(\rho_a, \rho_b)$)

$$g_n(x,t;\boldsymbol{\xi},\boldsymbol{\tau}) = a_n(x,t;\boldsymbol{\xi},\boldsymbol{\tau}) + b_n(x,t;\boldsymbol{\xi},\boldsymbol{\tau}),$$
$$G_n(x;\boldsymbol{\xi},\boldsymbol{s}) = A_n(x;\boldsymbol{\xi},\boldsymbol{s}) + B_n(x;\boldsymbol{\xi},\boldsymbol{s}).$$

Case (b): linear ($j=1$) and multilinear ($j \ge 2$) maps (with $\rho_g \ge \min_{1\le\ell\le j} \rho_{a^{[\ell]}}$)

$$g_n(x,t;\boldsymbol{\xi},\boldsymbol{\tau}) = \sum_{\substack{m\in(\mathbb{N}^*)^j \\ m_1+\cdots+m_j=n}} B^j\left[a_{m_1}^{[1]}(x,t;\sigma_m^1(\boldsymbol{\xi}),\sigma_m^1(\boldsymbol{\tau})),\ldots,a_{m_j}^{[j]}\left(x,t;\sigma_m^j(\boldsymbol{\xi}),\sigma_m^j(\boldsymbol{\tau})\right)\right], \tag{25}$$

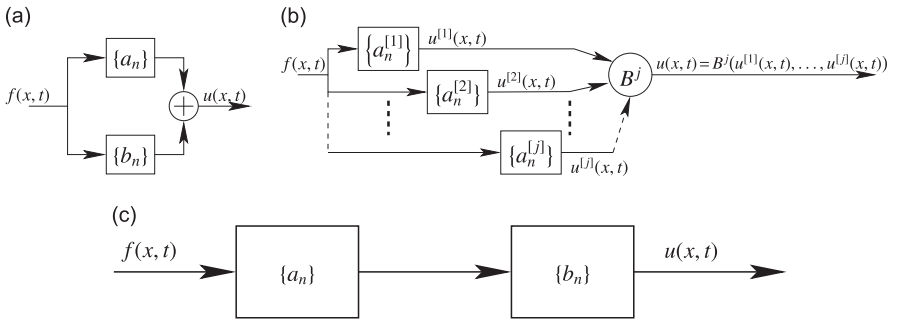

Fig. 4. Interconnection laws of several Green–Volterra systems: (a) sum, (b) linear and multilinear maps, and (c) cascade of two systems.

$$G_n(x;\boldsymbol{\xi},\boldsymbol{s}) = \sum_{\substack{m\in(\mathbb{N}^*)^j\\ m_1+\cdots+m_j=n}} B^j\left[A^{[1]}_{m_1}\left(x;\sigma^1_m(\boldsymbol{\xi}),\sigma^1_m(\boldsymbol{s})\right),\ldots,A^{[j]}_{m_j}\left(x;\sigma^j_m(\boldsymbol{\xi}),\sigma^j_m(\boldsymbol{s})\right);\right], \tag{26}$$

where for $m\in(\mathbb{N}^*)^j$ and $1\le\ell\le j$, the selection function $\sigma^\ell_m(\boldsymbol{\xi})=(\xi_{m_1+\cdots+m_{\ell-1}+1},\ldots,\xi_{m_1+\cdots+m_\ell})$ is introduced for the sake of conciseness. A simple example corresponds to the product of two outputs (bilinear map $B^2(a,b)=ab$). In this case Eqs. (25) and (26) reduce to $g_n(x,t;\boldsymbol{\xi},\boldsymbol{\tau})=\sum_{m=1}^{n-1}a^{[1]}_m(x,t;(\xi_1,\ldots,\xi_m),(\tau_1,\ldots,\tau_m))a^{[2]}_{n-m}(x,t;(\xi_{m+1},\ldots,\xi_n),(\tau_{m+1},\ldots,\tau_n))$ and a similar formula for G_n.

Note that B^j can also be replaced by a multilinear operator B^j_x which acts on the space variable, rather than a simple function. For space–time operators $B^j_{x,t}$, Eq. (25) is still valid, but not Eq. (26) which must be adapted. As a special case, if all series $\{a^{[\ell]}_n\}_{n\in\mathbb{N}^*}$ are the same, this adaptation can be derived by considering the cascade of two Green–Volterra series, as follows.

Case (*c*1): cascade of a nonlinear and a linear systems ($b_1\in\mathcal{G}_1$ and $b_n=0$ if $n\ge2$ so that $\rho_g=\rho_a$)

$$g_n(x,t;\boldsymbol{\xi},\boldsymbol{\tau}) = \int_{\Omega\times\mathbb{T}} b_1(x,t;y,\theta)a_n(y,\theta;\boldsymbol{\xi},\boldsymbol{\tau})\,\mathrm{d}y\,\mathrm{d}\theta, \tag{27}$$

$$G_n(x;\boldsymbol{\xi},\boldsymbol{s}) = \int_{\Omega} B_1(x;y,s_1+\cdots+s_n)A_n(y;\boldsymbol{\xi},\boldsymbol{s})\,\mathrm{d}y. \tag{28}$$

Case (*c*2): cascade (general case)

$$g_n(x,t;\boldsymbol{\xi},\boldsymbol{\tau}) = \sum_{j=1}^{n}\int_{\Omega^j\times\mathbb{T}^j}\sum_{\substack{m\in(\mathbb{N}^*)^j\\ m_1+\cdots+m_j=n}} b_j(x,t;\boldsymbol{y},\boldsymbol{\theta})a_{m_1}\left(y_1,\theta_1;\sigma^1_m(\boldsymbol{\xi}),\sigma^1_m(\boldsymbol{\tau})\right)\quad\ldots a_{m_j}\left(y_j,\theta_j;\sigma^j_m(\boldsymbol{\xi}),\sigma^j_m(\boldsymbol{\tau})\right)\mathrm{d}\boldsymbol{y}\,\mathrm{d}\boldsymbol{\theta},$$

$$G_n(x;\boldsymbol{\xi},\boldsymbol{s}) = \sum_{j=1}^{n}\int_{\Omega^j}\sum_{\substack{m\in(\mathbb{N}^*)^j\\ m_1+\cdots+m_j=n}} B_j\left(x;\boldsymbol{y},\chi_m(\boldsymbol{s})\right)A_{m_1}\left(y_1;\sigma^1_m(\boldsymbol{\xi}),\sigma^1_m(\boldsymbol{s})\right)\ldots A_{m_j}\left(y_j;\sigma^j_m(\boldsymbol{\xi}),\sigma^j_m(\boldsymbol{s})\right)\mathrm{d}\boldsymbol{y},$$

where for $m\in(\mathbb{N}^*)^j$, function $\chi_m(\boldsymbol{s})$ is the j-tuple, the ℓ coordinate of which is the sum of the selected Laplace variables $\sigma^\ell_m(\boldsymbol{s})$, that is, $\chi_m(\boldsymbol{s})=(\overline{\sigma^1_m(\boldsymbol{s})},\ldots,\overline{\sigma^j_m(\boldsymbol{s})})$ with $\overline{\sigma^\ell_m(\boldsymbol{s})}=\sum_{i=1}^{m_\ell}s_{m_1+\cdots+m_{\ell-1}+i}$.

3.4. Canceling system, principle of equivalence and solution kernels

This section describes a formal method to derive the Green–Volterra series $\{g_n\}_{n\in\mathbb{N}^*}$ of the system ($\mathcal{S}$) governed by (17) and (18), see Fig. 5(a). It is based on the use of interconnection laws and a canceling system, as proposed in [36, Section 2.2] for differential systems.

Introduce the system ($\mathcal{C}$) with input (u,f) and output $z=L_{x,t}[u]-f-K_{x,t}[u,f]$. Cascading ($\mathcal{S}$) and ($\mathcal{C}$) as in Fig. 5(b) defines the system ($\mathcal{Z}$) with input f and output z. As z is exactly zero for trajectories of system ($\mathcal{S}$), all the kernels $\{z_n\}$ of ($\mathcal{Z}$) are zero: we call ($\mathcal{C}$), the *canceling system* with respect to system ($\mathcal{S}$).

Exploiting interconnection laws (a) and (b), it follows that the kernels $z_n(x,t;\boldsymbol{\xi},\boldsymbol{\tau})$ of system ($\mathcal{Z}$) exactly involve the same combinatorics as in (19) and (20) and that, keeping the same notations,

$$(0=)z_n=L_{x,t}[g_n]-r_n\quad\text{with ((see Eq. (23)) } r_1(x,t;\xi_1,\tau_1)=\delta^1_{x,t}(\xi_1,\tau_1), \tag{29}$$

$$r_n(x,t;\boldsymbol{\xi},\boldsymbol{\tau}) = \sum_{\substack{(p,q)\in[0,n]^2_{\mathbb{N}}\\ 2\le p+q\le n}}\sum_{\substack{m\in(\mathbb{N}^*)^p\\ m_1+\cdots+m_p=n-q}} K^{p,q}_{x,t}\Big[g_{m_1}\left(x,t;\sigma^1_m(\boldsymbol{\xi}),\sigma^1_m(\boldsymbol{\tau})\right),\ldots,g_{m_p}\left(x,t;\sigma^p_m(\boldsymbol{\xi}),\sigma^p_m(\boldsymbol{\tau})\right),$$
$$\delta^1_{x,t}(\xi_{n-q+1},\tau_{n-q+1}),\ldots,\delta^1_{x,t}(\xi_n,\tau_n)]\quad\text{if } n\ge2, \tag{30}$$

where variables x and t of kernels g_{m_ℓ} are kept inside operator $K^{p,q}_{x,t}$, for the sake of legibility.

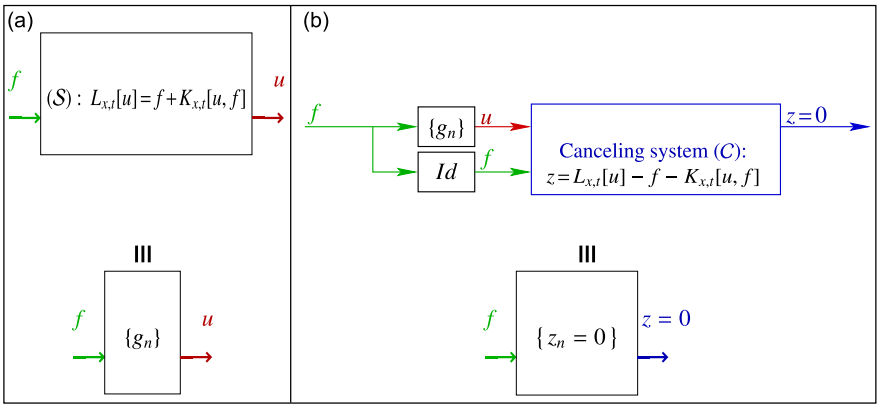

Fig. 5. Canceling system and equivalence principle of Green–Volterra kernels.

Remark 5 (*Interpretation*). In these equations, $L_{x,t}[g_n]$ are the Green–Volterra kernels of system with input f and output $L_{x,t}[u]$, and r_n are those for input f and output $f+K_{x,t}[u,f]$. Kernels $L_{x,t}[g_n]$ can be obtained by using, either the interconnection law (b) for $j=1$ with $B^1_{x,t}=L_{x,t}$ and $a_n=g_n$, or the law (c1) with $a_n=g_n$ and choosing b_1 to be the (linear) kernel associated with the linear operator $L_{x,t}$. Kernels r_n are sums (law (a)) of multilinear operators (law (b)), in which the last q Dirac distributions are the kernels of identity (ahead of ($\mathcal{C}$) in Fig. 5(b)).

For $n=1$, the solution of (29) with $z_1=0$ exactly yields Green's function of the linearized problem (Eq. (17) with $K_{x,t}\equiv 0$). For $n\geq 2$, solving iteratively the sequence of linear problems (29) and (30), still with $z_n=0$, yields the Green–Volterra kernels

$$g_n(x,t;\boldsymbol{\xi},\boldsymbol{\tau})=\int_{\Omega\times\mathbb{T}} g_1(x,t;y,\theta)r_n(y,\theta;\boldsymbol{\xi},\boldsymbol{\tau})\,\mathrm{d}y\,\mathrm{d}\theta. \tag{31}$$

Remark 6 (*Canceling system and transfer kernels in practice*). For many applications, $K_{x,t}$ is a finite sum of multilinear operators. This leads to a less complex combinatorics as above. Moreover, for time-invariant systems, using transfer kernels makes equations simpler: the integrals w.r.t. time variables become algebraic relations w.r.t. Laplace variables. In practice, these algebraic relations are precisely used in Section 4, to compute closed-form formulae of the transfer kernels.

3.5. Realization

As mentioned after Eq. (21), u_n is exactly the term of order n of Eq. (22): the regular perturbation method (Section 3.1) yields the same solution u as the Green–Volterra series (Section 3.2), the kernels g_n of which fully characterize the system independent of the input (as Green's function does for a linear problem). Eq. (31) with (30), or alternatively Eq. (21) with (20), leads to the realization (in the sense of system theory, see [14, Chapter 4]) described by the block-diagram in Fig. 6 (limited to the three first orders only).

Thus, simulations can be built using finite-dimensional discrete-time approximate versions of a linear operator $\mathfrak{G}_1$ (see Fig. 6) and (finite dimensional versions of) multilinear operators $K^{p,q}_{x,t}$.

As there are no feedback loops (no implicit equations) in Fig. 6, only explicit calculations are needed. Moreover, the stability is exclusively conditioned by that of (the discrete-time version of) $\mathfrak{G}_1$ and (only if multilinear operators depend on time) that of $K_{x,t}$.

4. Application to the Kirchhoff model of the string

4.1. Linear and multilinear operators

The nonlinear Kirchhoff model given by Eqs. (1)–(3) in Section 2 has the general form equations (17) and (18) in Section 3. The linear operator $L_{x,t}$ is

$$L_{x,t}=\partial_t^2+2\alpha\partial_t-\partial_x^2 \quad \text{in } \Omega\times\mathbb{T} \quad \text{with } \Omega=]0,1[\quad \text{and} \quad \mathbb{T}=\mathbb{R}_+, \tag{32}$$

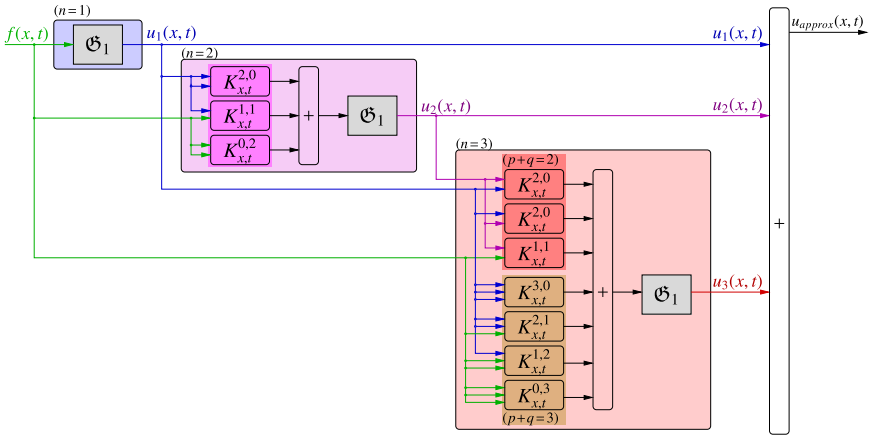

Fig. 6. Realization of the three first orders of the general structure obtained from Eqs. (19) to (20) and from (29) to (30). In this structure, blocks $K_{x,t}^{p,q}$ are the multilinear operators in Eq. (18), fed by the $p+q$ signals, from top to bottom. Blocks (with no rounded corners) correspond to the linear operator $\mathfrak{G}_1$ associated with Green's function g_1, that is, $\mathfrak{G}_1[w](x,t)=\int_{\Omega\times\mathbb{T}} g_1(x,t;\xi,\tau)w(\xi,\tau)\,\mathrm{d}\xi\,\mathrm{d}\tau$.

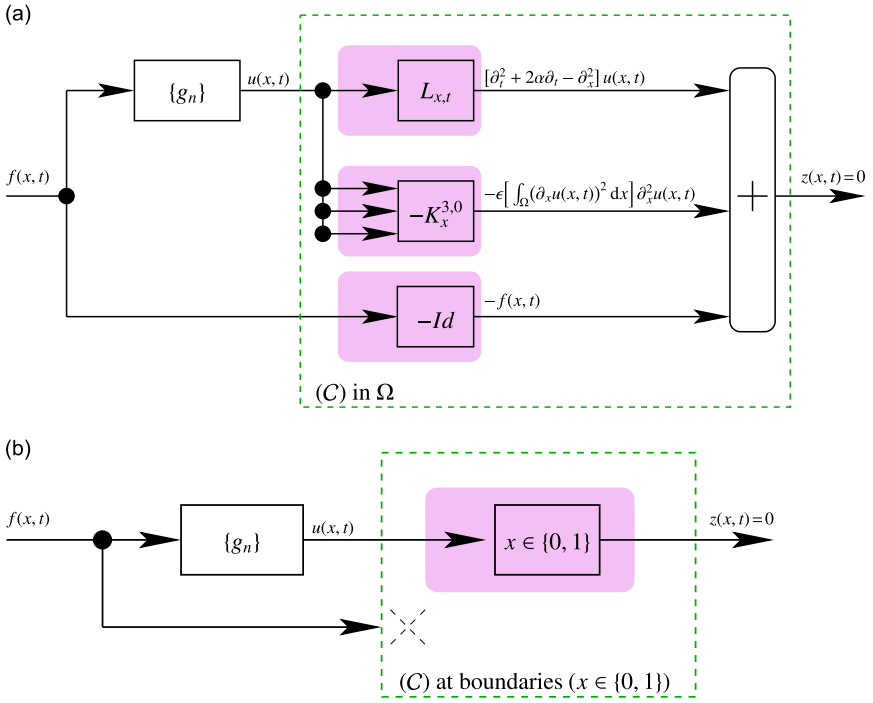

Fig. 7. Block-diagram versions of Eq. (1) (a) and of Eq. (2) (b) for a general force $f(x,t)$. The associated canceling systems are delimited by dotted boxes.

with Dirichlet boundary conditions and zero initial conditions. The nonlinear operator $K_{x,t}$ defined by Eq. (18) is reduced to the space-operator $(u,f)\mapsto K_{x,t}[u,f]=K_x^{3,0}[u,u,u]$ with

$$K_x^{3,0}[a,b,c]=\varepsilon\left[\int_\Omega \partial_x a(x)\partial_x b(x)\,\mathrm{d}x\right]\partial_x^2 c(x). \tag{33}$$

4.2. Canceling system and Green–Volterra transfer kernels

Denote by $\{g_n\}_{n\in\mathbb{N}^*}$ the Green–Volterra series of the nonlinear Kirchhoff model. As this model is time-invariant, according to Property 2, introduce the corresponding transfer kernels G_n defined from g_n by Eq. (24). Using the interconnection laws to

rewrite the appropriate canceling system (see Fig. 7) in the Laplace domain leads to a Laplace version of Eqs. (29) and (30). Eq. (29) becomes, for all $n \in \mathbb{N}^*$ and $\boldsymbol{s} \in (\mathbb{C}_0^+)^n$,

$$[\Gamma(s_1+\cdots+s_n)^2-\partial_x^2]G_n(x;\boldsymbol{\xi},\boldsymbol{s})=R_n(x;\boldsymbol{\xi},\boldsymbol{s}) \quad \text{on the string } (x\in\Omega), \tag{34}$$

and

$$G_n(x;\boldsymbol{\xi},\boldsymbol{s})=0 \quad \text{at boundaries } (x\in\{0,1\}), \tag{35}$$

where Γ is still defined by Eq. (9) so that the first member of Eq. (34) effectively corresponds to the cascade of $\{g_n\}$ and the linear operator $\partial_t^2+2\alpha\partial_t-\partial_x^2$ (see Fig. 7(a)) with Dirichlet boundary conditions (see Fig. 7(b)). Transfer kernels R_n are the Laplace transforms of $\underline{r}_n(x;\boldsymbol{\xi},\boldsymbol{\theta})=r_n(x,0;\boldsymbol{\xi},-\boldsymbol{\theta})$ (see Property 2). This yields

$$R_1(x;\xi_1,s_1)=\delta_x(\xi_1). \tag{36}$$

Moreover, according to Remark 5 and using the Laplace versions of interconnection laws (a) and (b), Eq. (30) becomes, for $n\geq 2$,

$$\begin{aligned}R_n(x;\boldsymbol{\xi},\boldsymbol{s})=&\sum_{\substack{m\in(\mathbb{N}^*)^3\\ m_1+\cdots+m_3=n}} K_x^{3,0}\left[G_{m_1}\left(x;\sigma_m^1(\boldsymbol{\xi}),\sigma_m^1(\boldsymbol{s})\right),G_{m_2}\left(x;\sigma_m^2(\boldsymbol{\xi}),\sigma_m^2(\boldsymbol{s})\right),\right.\\ &\left.G_{m_3}\left(x;\sigma_m^3(\boldsymbol{\xi}),\sigma_m^3(\boldsymbol{s})\right)\right]\\ =&\varepsilon\int_\Omega\left(\sum_{\substack{p,q,r\geq 1\\ p+q+r=n}}\partial_x G_p\left(x;\xi_1,\ldots,\xi_p,s_1,\ldots,s_p\right)\right.\\ &\left.\times\partial_x G_q(x;\xi_{p+1},\ldots,\xi_{p+q},s_{p+1},\ldots,s_{p+q})\right)\mathrm{d}x\\ &\times\partial_x^2 G_r(x;\xi_{p+q+1},\ldots,\xi_n,s_{p+q+1},\ldots,s_n).\end{aligned} \tag{37}$$

Eqs. (34) and (35) define a sequence of boundary problems indexed by $n\in\mathbb{N}^*$, which are differential w.r.t. x and linear w.r.t. G_n. Indeed, for any fixed n, Eqs. (36) and (37) only involve transfer kernels G_m of order $m<n$. Moreover, Eqs. (34) and (35) exactly restore Eqs. (7) and (8) with solution Eqs. (10) and (11), in which for all $\boldsymbol{\xi}\in\Omega^n$ and $\boldsymbol{s}\in(\mathbb{C}_0^+)^n$, function $x\mapsto U(x,s)$ is replaced by $x\mapsto G_n(x;\boldsymbol{\xi},\boldsymbol{s})$, $x\mapsto F(x,s)$ by $x\mapsto R_n(x;\boldsymbol{\xi},\boldsymbol{s})$, and $\Gamma(s)$ by $\Gamma(s_1+\cdots+s_n)$. Finally, it follows that the Green–Volterra transfer kernels are given by, for all $n\in\mathbb{N}^*$, $x\in\Omega$, $\boldsymbol{\xi}\in\Omega^n$ and $\boldsymbol{s}\in(\mathbb{C}_0^+)^n$,

$$G_1(x;\xi_1,s_1)=G(x;\xi_1,s_1) \quad \text{and, if } n\geq 2, G_n(x;\boldsymbol{\xi},\boldsymbol{s})=\int_\Omega G(x;y,s_1+\cdots+s_n)R_n(y;\boldsymbol{\xi},\boldsymbol{s})\,\mathrm{d}y, \tag{38}$$

where G is Green's function of the linearized problem, defined in the Laplace domain by Eq. (11).

Remark 7 (*Nonzero kernels*). As $K_{x,t}$ is composed of a multilinear operator of odd order, it follows that all the Green–Volterra kernels of even order are zero.

4.3. Modal decomposition and simulation in the time domain

The transfer kernels $x\mapsto G_n(x;\boldsymbol{\xi},\boldsymbol{s})$ can be decomposed on the orthonormal Hilbert basis $\{e_k\}_{k\in\mathbb{N}^*}$. More generally, this is also the case of $(x,\boldsymbol{\xi})\mapsto G_n(x;\boldsymbol{\xi},\boldsymbol{s})$ on the orthonormal Hilbert basis $\{e^{1+n}_{k,\ell_1,\ldots,\ell_n}\}_{(k,\ell_1,\ldots,\ell_n)\in(\mathbb{N}^*)^{1+n}}$ of $L^2(\Omega^{1+n})(\equiv(L^2(\Omega^{1+n}))^{n+1}$ endowed with the 2-norm) where

$$e^{1+n}_{k,\ell_1,\ldots,\ell_n}(x,\boldsymbol{\xi})=[e_k\otimes e_{\ell_1}\otimes\cdots\otimes e_{\ell_n}](x,\xi_1,\ldots,\xi_n).$$

For $n=1$, Eqs. (36) and (38) lead to

$$G_1(x;\xi_1,s_1)\underset{L^2(\Omega^2)}{=}\sum_{k=1}^{+\infty}G^{[k]}(s_1)e^2_{k,k}(x,\xi_1), \tag{39}$$

so that only the terms corresponding to "diagonal bi-modes" $e^2_{k,k}$ are nonzero. Notice that this is in accordance with solution (12) and (13) and is due to the orthogonality of eigenfunctions e_j's.

By induction, this result is straightforwardly generalized as follows: for all $n\in\mathbb{N}^*$, $x\in\Omega$ and $(\boldsymbol{\xi},\boldsymbol{s})\in(\Omega\times\mathbb{C}_0^+)^n$,

$$\begin{aligned}G_n(x;\boldsymbol{\xi},\boldsymbol{s})&\underset{L^2(\Omega^{1+n})}{=}\sum_{k=1}^{+\infty}G_n^{[k]}(\boldsymbol{s})e^{1+n}_{k,\ldots,k}(x,\boldsymbol{\xi}).\\ \text{with } G_n^{[k]}(\boldsymbol{s})&=G^{[k]}(s_1+\cdots+s_n)R_n^{[k]}(\boldsymbol{s}),\\ R_1^{[k]}(s_1)&=1,\end{aligned}$$

if $n\geq 2$,

$$R_n^{[k]}(\boldsymbol{s})=-\varepsilon k^2\pi^4\sum_{\substack{p,q,r\geq 1\\ p+q+r=n}}\left[\sum_{\ell=1}^{+\infty}\ell^2 G_p^{[\ell]}(s_1,\ldots,s_p)G_q^{[\ell]}(s_{p+1},\ldots,s_{p+q})\right]G_r^{[k]}\left(s_{p+q+1},\ldots,s_n\right).$$

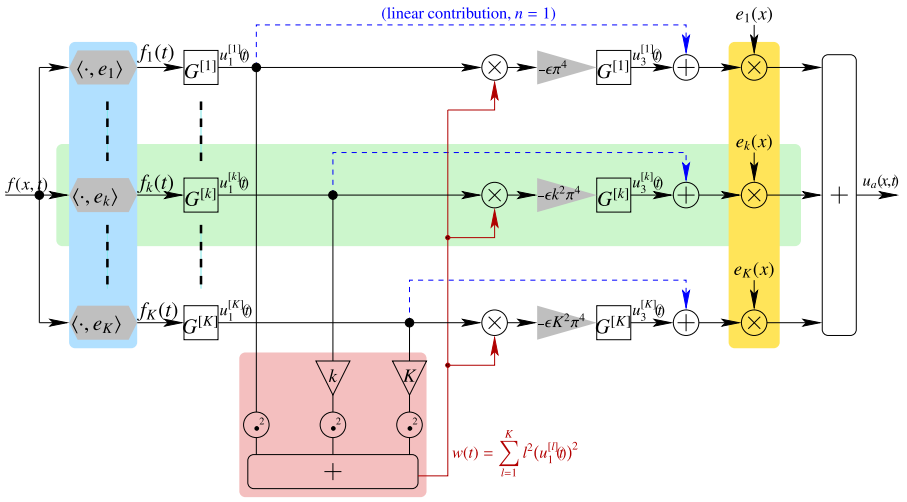

Fig. 8. Block-diagram of an $o(\varepsilon)$−simulation of Eq. (1) based on the Green–Volterra kernels with K modes: the excitation force $f(x,t)$ is completely unknown to the system and is decomposed on the modal basis using a scalar product.

The first nonzero kernels for $n \geq 2$ correspond to

$$\begin{aligned} G_3^{[k]}(s_1,s_2,s_3) &= G^{[k]}(s_1+s_2+s_3)R_3^{[k]}(s_1,s_2,s_3) \\ &= -\varepsilon k^2\pi^4 G^{[k]}(s_1+s_2+s_3)\sum_{\ell=1}^{+\infty}\ell^2 G_1^{[\ell]}(s_1)G_1^{[\ell]}(s_2)G_1^{[k]}(s_3) \\ &= -\varepsilon k^2\pi^4 G^{[k]}(s_1+s_2+s_3)\sum_{\ell=1}^{+\infty}\ell^2 G^{[\ell]}(s_1)G^{[\ell]}(s_2)G^{[k]}(s_3) \end{aligned}$$

$$\begin{aligned} G_5^{[k]}(s_1,\ldots,s_5) &= G^{[k]}(s_1+\cdots+s_5)R_5^{[k]}(s_1,\ldots,s_5) \\ &= -\varepsilon k^2\pi^4 G^{[k]}(s_1+\cdots+s_5)\sum_{\substack{p,q,r\geq 1\\ p+q+r=5}}\sum_{\ell=1}^{+\infty}\ell^2 G_p^{[\ell]}(s_1,\ldots,s_p) \\ &\quad\times G_q^{[\ell]}(s_{p+1},\ldots,s_{p+q})G_r^{[k]}(s_{p+q+1},\ldots,s_5). \end{aligned}$$

Using previous work (Section 2.3), the Green–Volterra kernels modal projections can be identified to be the same structure presented in Fig. 2. Indeed, for $n=1$, the Green–Volterra kernel is Green's function (cf. Eq. (14)), and for $n \geq 2$, the kernels consist in sums and products of the output of this already known Green's function.

Hence, for a general excitation $f(x,t)$, the simulation is performed using the structure displayed in Fig. 8. It actually corresponds to the "intuitive solution" mentioned at the end of Section 2.3: the only difference with the previous work (recalled in Fig. 2) for excitations of type Eq. (15) is that ϕ_k must be replaced by the modal projection $\langle\cdot, e_k\rangle$.

Remark 8. Fig. 8 corresponds to the particular case of Fig. 6 in which the only nonzero multilinear operator $K_x^{3,0}$ is detailed and expanded on the K first modes of the string.

5. Realizations and discussion

In the following section, results are presented for the *dimensionless* string model described in Eq. (1). The string length is therefore defined in $\Omega =]0,1[$.

Figs. 9 and 10 represent the time response of the string at an observation point $x=0.57$. The excitation force is defined by $f(x,t) = \psi(x,t) f_{\max} t/T_{\text{force}}$ for $t \in [0, T_{\text{force}}]$ where $f_{\max}$ is the maximum amplitude of the force and $T_{\text{force}} = 0.01$ s. The spatial distribution of the force is a cosine moving thanks to the function ψ defined by

$$\psi(x,t) = \cos\left(\pi\frac{(x-x_0+0.2t)}{\ell}\right) \quad \text{if } |x-x_0+0.2t| < \frac{\ell}{2} \quad \text{and} \quad \psi(x,t)=0 \quad \text{otherwise} \tag{40}$$

where the value of ℓ corresponds to 4 percent of the string length.

The sampling frequency is $f_s = 44\,100$ Hz and the number of modes is $K=20$. The same conclusions can be made in comparison with [21], i.e. the approximation at a given order of nonlinearity (here $N=5$) is valid until a maximum of force

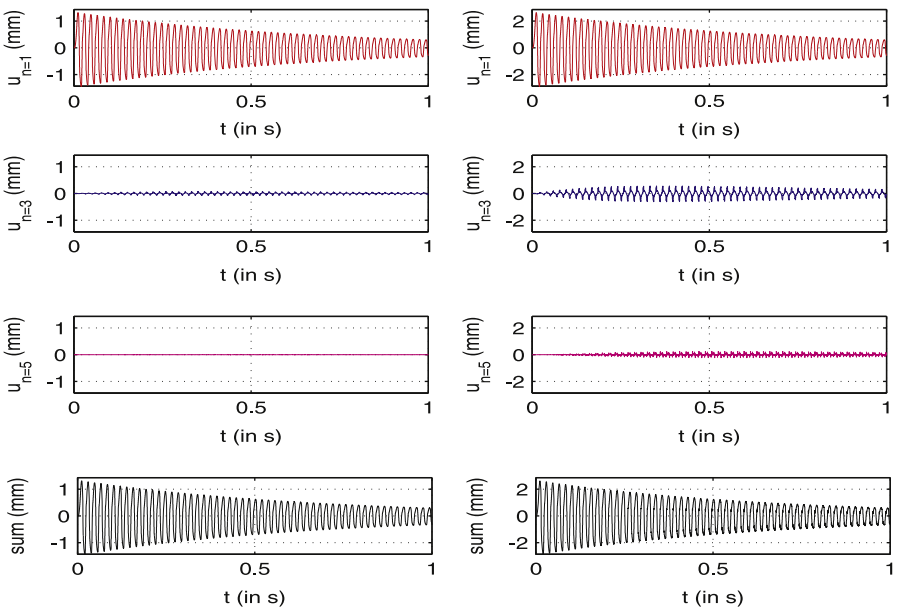

Fig. 9. Simulation of Eq. (1) for $f^1_{\max} = 5$ N: linear approximation is correct since the amplitude of the transverse displacement is very small. For $f^2_{\max} = 10$ N, nonlinear effects begins to appear mainly for order 3.

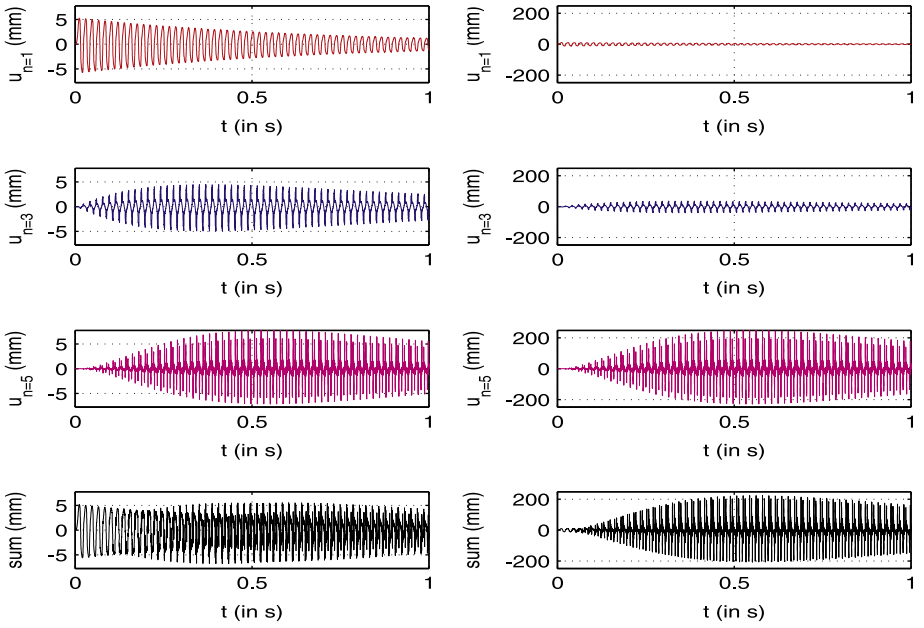

Fig. 10. Simulation of Eq. (1) for $f^3_{\max} = 20$ N: the nonlinear responses have the same amplitude that the linear one, $f^3_{\max}$ is roughly the convergence radius of the Volterra series. For $f^4_{\max} = 40$ N, the amplitude of the force is too high, the series does not converge anymore.

amplitude (here $F^3_{\max}$), where the nonlinear response has the same magnitude than the linear one. Without a calculation of the convergence radius, this is a good observation to define a valid range of excitation force.

Fig. 11 presents the string transverse displacement when the force is nonzero. It shows the purpose of Green–Volterra kernels, in comparison with previous works, i.e. the spatial variation of the force $f(x,t)$ along the string using the function $\psi(x,t)$.

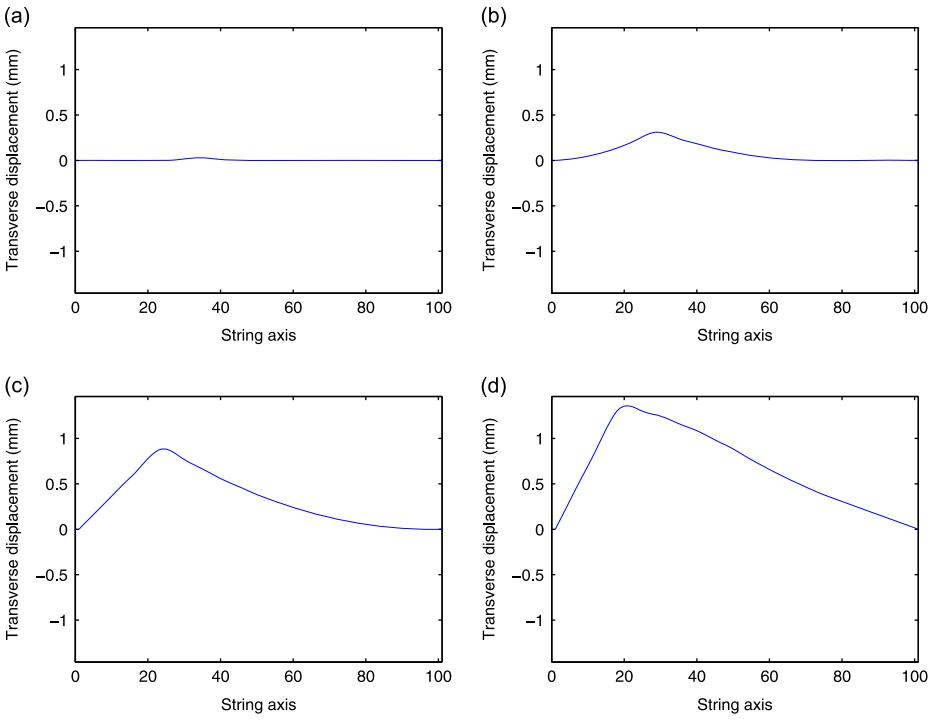

Fig. 11. Transverse displacement of the string excited by the force $f(x,t)=\psi(x,t)f_{\max}t/T_{\text{force}}$ where ψ is defined by Eq. (40) at four times: (a) 50 samples, (b) 150 samples, (c) 250 samples and (d) 350 samples.

6. Conclusion

This paper has presented the calculation of Green–Volterra kernels for the Kirchhoff string model. The definition of the kernels is provided, in relation with Green's function of the linearized problem. The method is then the following:

- build the canceling system from the physical model;
- derive linear equations satisfied by the Green–Volterra kernels, using the interconnection laws;
- write a structure of simulation based on the discrete-time version of the linear operator, and instantaneous sums and products (or multilinear operators).

This formalism allows one to use Green's function properties to compute the dynamics of a weakly nonlinear problem of type Eqs. (17) and (18) with an excitation force $f(x,t)$. The main result of the computation is the possibility to use a nontime-invariant space repartition of the force. This extends Green's formalism to weakly nonlinear problems. Moreover, the structure of simulation is very similar to the particular case $\phi(x)f_{\text{tot}}(t)$.

However, the convergence of the Green–Volterra series has not been studied in this paper. This will be addressed in a future work, based on studies proposed in e.g. [32–33]. Here, in order to have proper approximations in practice, the amplitude of the force is limited so that the nonlinear response has a lower magnitude than the linear one.

This generalization of an excitation force $f(x,t)$ is an important step to get more general results in the synthesis of nonlinear models. It will allow one to deal with other kinds of problems. For instance, contact problems for deformable solids need to use variable force (in space and time) to represent the interaction between two solids at the contact surface. The Green–Volterra kernels could be used to represent each solid. This will require to work on more elaborated physical models (e.g. beams or plates) in order to highlight the possibilities regarding the excitation force.

References

[1] G. Gorain, S. Bose, Uniform stability of damped nonlinear vibrations of an elastic string, *Proceedings of the Indian Academy of Sciences—Mathematical Sciences* 113 (2003) 443–449.
[2] G. Kirchhoff, *Vorlesungen Über Mathematische Physik: Mechanik*, Leipzig, Teubner, 1877.
[3] C. Touzé, Analyse et modélisation de signaux acoustiques et vibratoires chaotiques. Application aux instruments de percussion non-linéaires, PhD Thesis, ENST, 2000.
[4] A. Watzky, Non-linear three-dimensional large-amplitude damped free vibration of a stiff elastic stretched string, *Journal of Sound and Vibration* 153 (1992) 125–142.
[5] C. Valette, C. Cuesta, *Mécanique de la corde vibrante*, Hermès, 1993.
[6] G. Carrier, On the non-linear vibration problem of the elastic string, *Quarterly of Applied Mathematics* 3 (1945) 157–165.

[7] G. Anand, Large-amplitude damped free vibration of a stretched string, *Journal of the Acoustical Society of America* 45 (5) (1969) 1089–1096.
[8] A. Chaigne, V. Doutaut, Numerical simulations of xylophones. I. Time-domain modeling of the vibrating bars, *Journal of the Acoustical Society of America* 101 (1997) 539–557.
[9] S. Bilbao, J.O. Smith, Energy-conserving difference schemes for nonlinear strings, *Acta Acustica United with Acustica* 91 (2005) 299–311.
[10] J.O. Smith, Virtual acoustic musical instruments: review of models and selected research, *Workshop on Applications of Signal Processing to Audio and Acoustics* (*WASPAA*), IEEE.
[11] V. Volterra, *Theory of Functionals and of Integral and Integro-Differential Equations*, Dover Publications, 1959.
[12] R.W. Brockett, Volterra series and geometric control theory, *Automatica* 12 (1976) 167–176.
[13] E.G. Gilbert, Functional expansions for the response of nonlinear differential systems, *IEEE Transactions on Automatic Control* 22 (1977) 909–921.
[14] W.J. Rugh, *Nonlinear System Theory, the Volterra/Wiener Approach*, The Johns Hopkins University Press, Baltimore, 1981.
[15] M. Fliess, Fonctionnelles causales non linéaires et indéterminées non commutatives, *Bulletin de la SMF* 109 (1981) 3–40.
[16] M. Fliess, M. Lamnabhi, F. Lamnabhi-Lagarrigue, An algebraic approach to nonlinear functional expansions, *IEEE Transactions on Circuits and Systems* 30 (1983) 554–570.
[17] P.E. Crouch, P.C. Collingwood, The observation space and realizations of finite Volterra series, *SIAM Journal on Control and Optimization* 25 (1987) 316–333.
[18] M. Schetzen, *The Volterra and Wiener Theories of Nonlinear Systems*, Wiley-Interscience, 1989.
[19] F. Lamnabhi-Lagarrigue, Analyse des Systèmes Non Linéaires, Editions Hermès, 1994. ISBN: 2-86601-403-0.
[20] A. Isidori, *Nonlinear Control Systems*, 3rd edition, Springer Verlag, 1995.
[21] T. Hélie, D. Roze, Sound synthesis of a nonlinear string using Volterra series, *Journal of Sound and Vibration* 314 (2008) 275–306.
[22] A. Chaigne, J. Kergomard, *Acoustique des Instruments de Musique*, Berlin, 2008.
[23] G. Green, *An Essay on the Application—Mathematical Analysis to the Theories of Electricity and Magnetism*, T. Wheelhouse, Nottingham, UK, 1828.
[24] A.D. Polyanin, *Handbook of Linear Partial Differential Equations for Engineers and Scientists*, Chapman & Hall/CRC Press, Boca Raton, 2002.
[25] J. Bensoam, Représentation intégrale appliquée à la synthèse sonore par modélisation physique, PhD Thesis, Université du Maine, 2003.
[26] L. Schwartz, Méthodes mathématiques pour les sciences physiques, Hermann, 1965.
[27] R. Caussé, J. Bensoam, N. Ellis, Modalys, a physical modeling synthesizer: more than twenty years of researches, developments, and musical uses, *Journal of the Acoustical Society of America*130–134, (2011) 2365–2365.
[28] H.K. Khalil, *Nonlinear Systems*, 3rd edition, Prentice Hall, 2002.
[29] H.-X. Li, C. Qi, Y. Yu, A spatio-temporal Volterra modeling approach for a class of distributed industrial processes, *Journal of Process Control* 19 (2009) 1126–1142.
[30] S. Boyd, L.O. Chua, C.A. Desoer, Analytical foundations of Volterra series, *IMA Journal of Mathematical Control and Information* 1 (1984) 243–282.
[31] A. Pazy, *Semigroups of Linear Operators and Applications to Partial Differential Equations*, Springer, 1983.
[32] T. Hélie, B. Laroche, Convergence of series expansions for some infinite dimensional nonlinear systems, *IFAC SSSC*, Vol. 4, Ancone, Italie, pp. 1–7.
[33] T. Hélie, B. Laroche, Series expansion of infinite dimensional linear-analytic systems: application to a nonlinear Euler–Bernoulli Beam. Technical Report 2013-1, Technical Report, INRA, 2013.
[35] M. Hasler, Phénomènes non linéaires, École Polytechnique Fédérale de Lausanne, 1999.
[36] T. Hélie, Modélisation physique d'instruments de musique et de la voix: systèmes dynamiques, problèmes directs et inverses, Technical Report, Habilitation à Diriger des Recherches, Université Pierre et Marie Curie, 2013.